Supporting Information

for

Exploring the Role of Inorganic and Organic Interfaces on CO_2 and CH_4 Partitioning: Case Study of Silica, Illite, Calcite and Kerogen Nanopores on Gas Adsorption and Nano-Scale Transport Behaviors

Sohaib Mohammed[1] and Greeshma Gadikota[1]*

[1]School of Civil and Environmental Engineering, Cornell University, 117 Hollister Hall, 527 College Avenue, Ithaca, NY 14853

[*] Corresponding Author. Phone: +1 608-262-0365. E-mail: gg464@cornell.edu

S1. Models, forcefields and initial configurations

The inorganic surfaces were constructed based on well-studies unit cells. Calcite surface with dimensions of 7.287 nm x 7.984 nm x 4.857 nm was built from a unit cell of (1 0 4) crystallographic face. Similarly, the silica surfaces were modeled by cutting along the (1 1 1) face of □-cristobalite SiO_2 crystal. The X, Y, and Z dimensions of the silica surface are 7.248 nm x 7.906 nm x 4.4251 nm, respectively. The illite unit cell was constructed using the formula of $K_{x+1}[Si_{(8-x)}Al_x][Al_{(4-x)}Mg_x]O_{20}(OH)_4$ (x=1) [1]. The unit cell was replicated in all directions to form a surface with dimensions of 7.273 nm x 7.943 nm x 4.698 nm.

The initial configurations were constructed as following:

a. Replicate calcite, silica and illite surfaces with the desired dimensions.
b. Extend the constructed surface along x-axis for 10 nm to construct the gas reservoir and fill the gas reservoir with 0.8 g/cm^3 of CO_2/CH_4 to match the density of the shale fluids[2].
c. Extend the generated cell in (c) in x-axis by 8 nm and fill the generated space with 1.24 g/cm^3 to match the kerogen matrix density[3].
d. Double the generated cell along z-axis with a separation distance of 2, 4 and 6 nm to represent the nanopores.

The construction steps of the initial configurations are shown **Figure S1**.

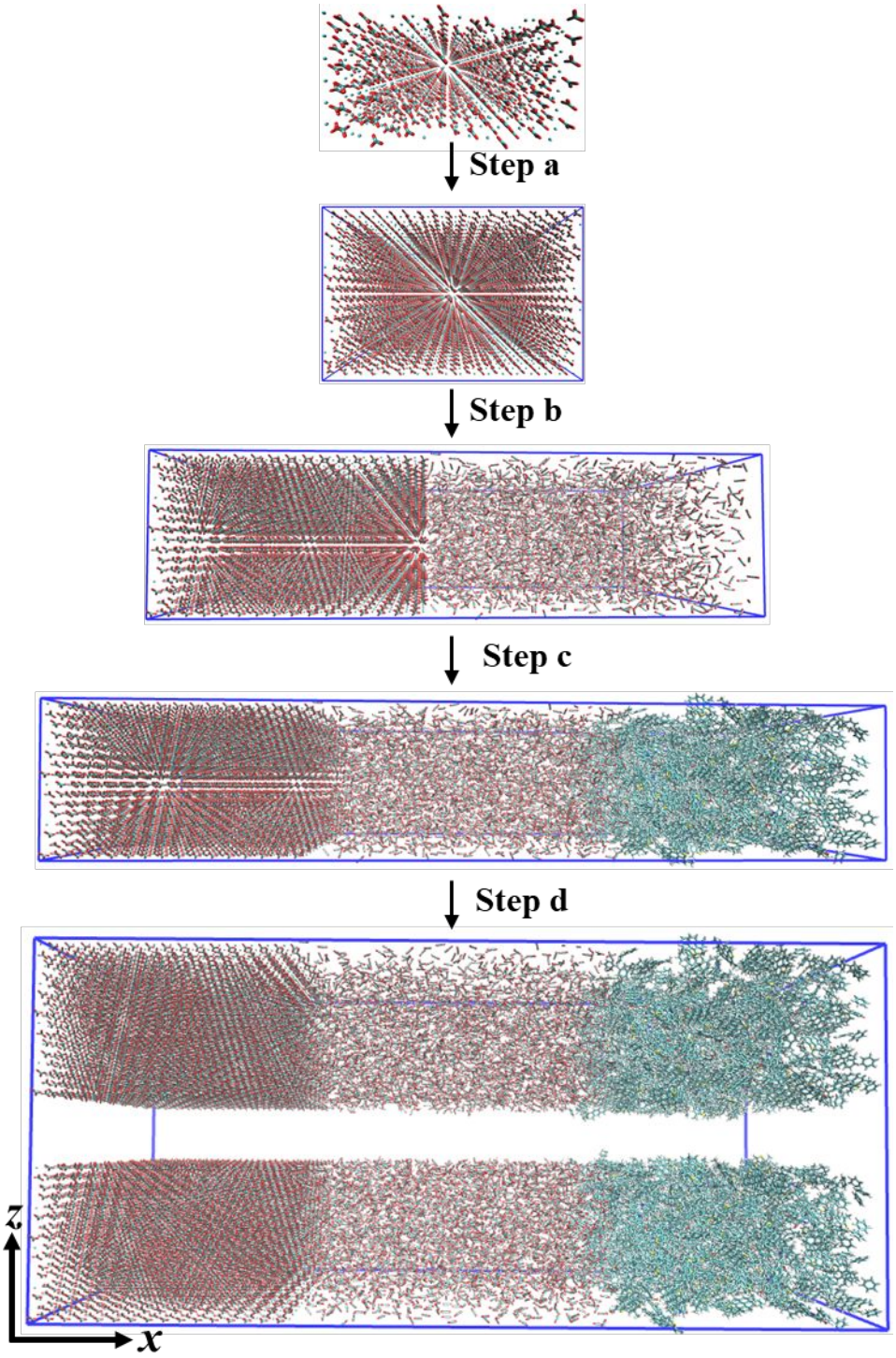

Figure S1. The construction steps of the initial configurations.

S2. The orientation of the adsorbed molecules

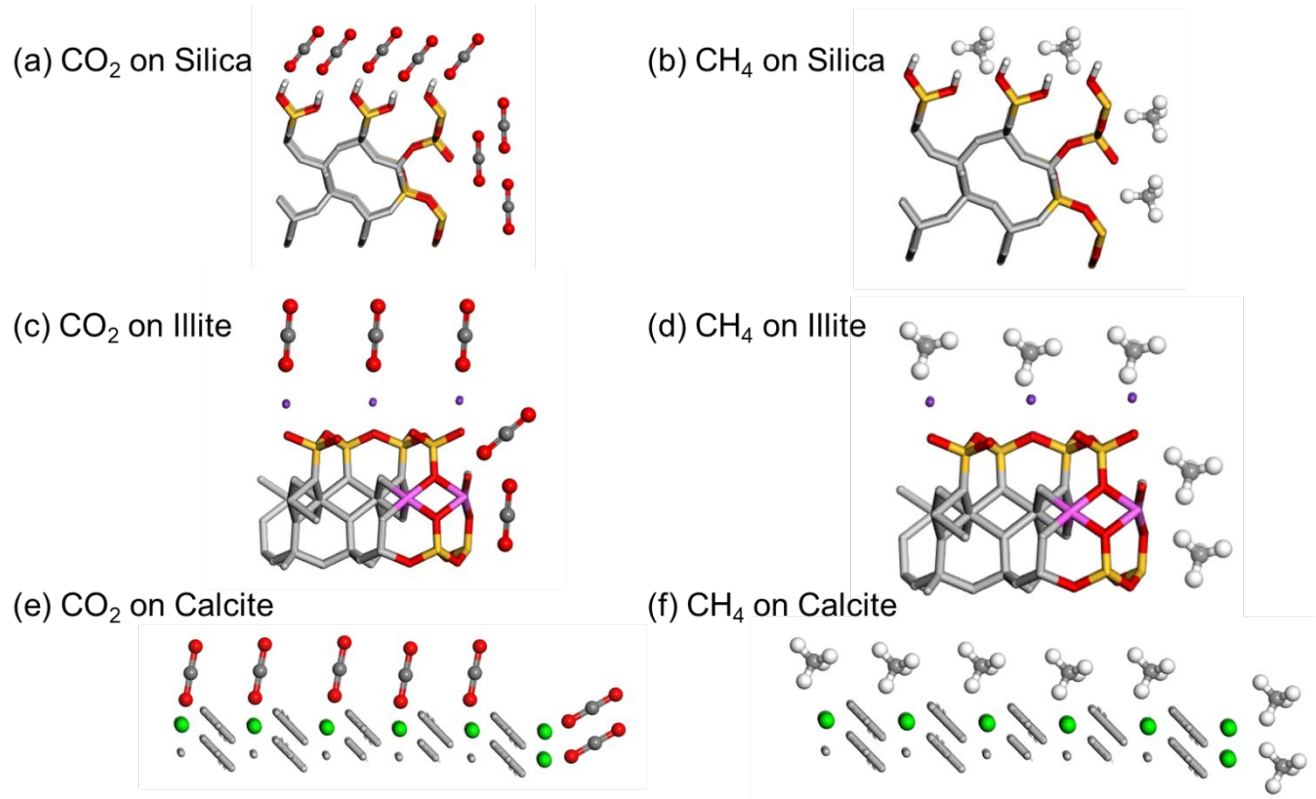

Figure S2. The orientation of the adsorbed CO_2 and CH_4 molecules on the surface and edges of silica (a and b), illite (c and d) and calcite (e and f).

S3. Density profiles

The density profiles of CO_2 and CH_4 with the axis normal to the pore surfaces (z-axis) are shown in **Figures S3 and S4**. CO_2 and CH_4 show a preferential adsorption on the internal pore surfaces and the partitioning of the gases molecules inside the kerogen matrices are also evident from **Figures S3 and S4**.

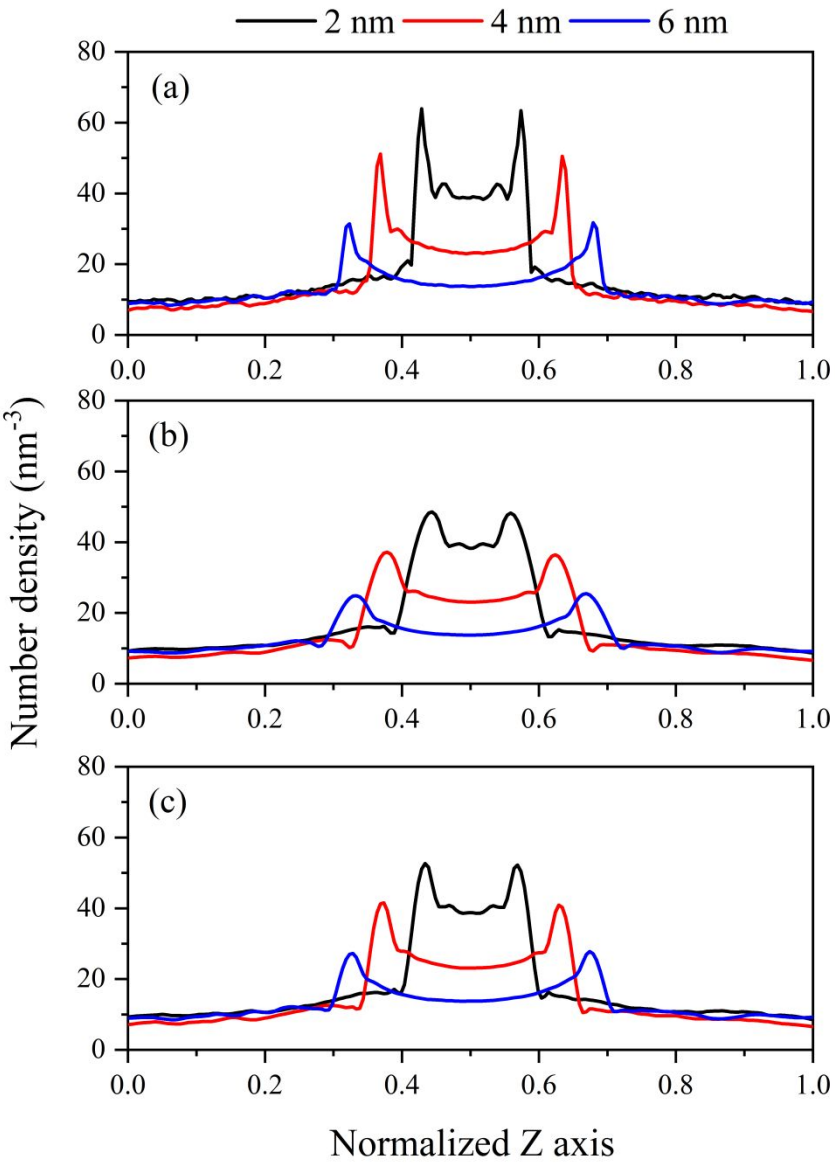

Figure S3. The density profile of CO_2 in the systems composed of kerogen and (a) calcite, (b) silica and (c) illite along the axis normal on the nanopores surface (z axis).

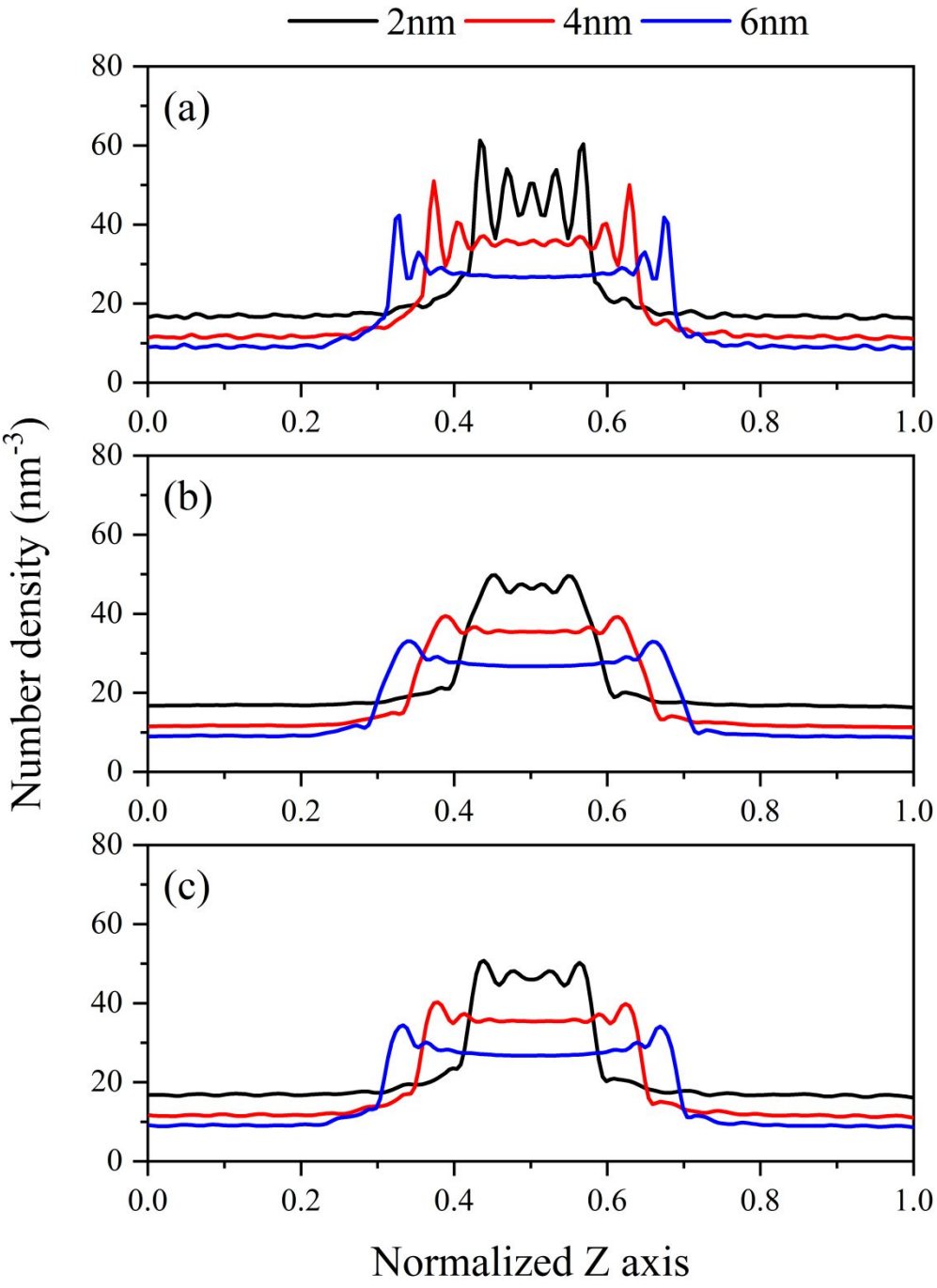

Figure S4. The density profile of CH_4 in the systems composed of kerogen and (a) calcite, (b) silica and (c) illite along the axis normal on the nanopores surface (z axis).

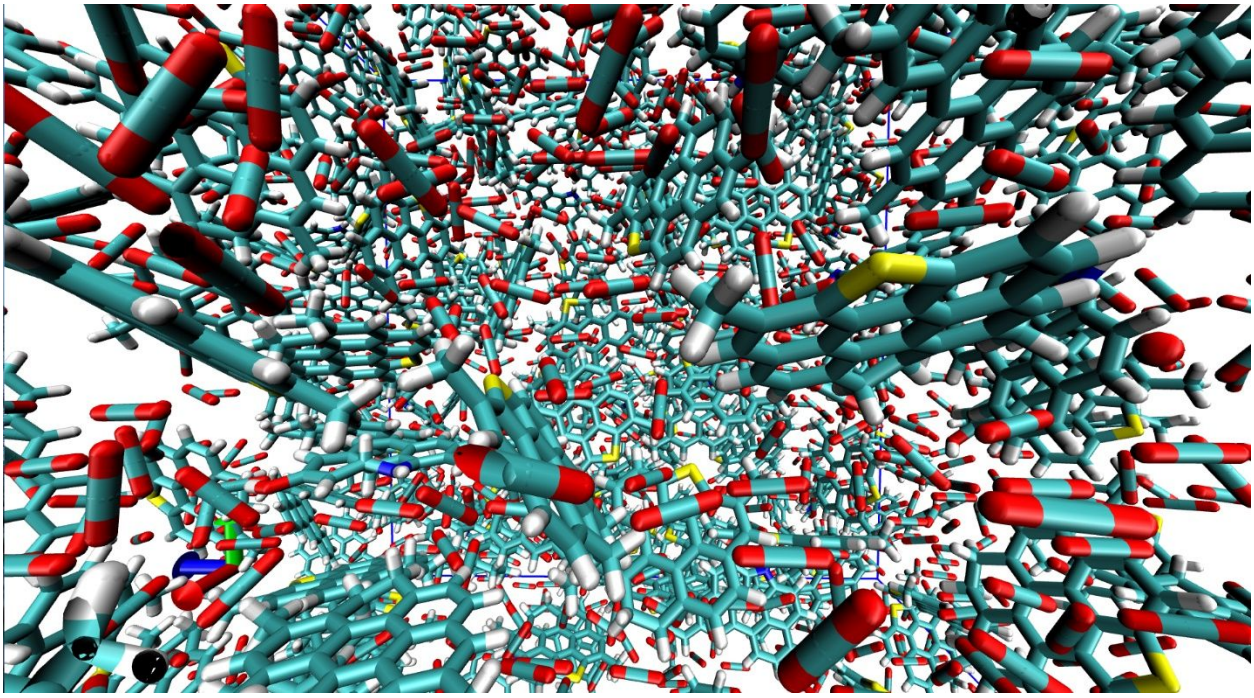

Figure S5. Snapshot for the kerogen intrinsic pores and the adsorbed CO_2 molecules within the kerogen matrix.

S4. The self-assembly of the kerogen fragments

Separate set of simulations are performed to quantify the self-assembly of kerogen fragments in the presence and absence of silica, illite and calcite surfaces. In the absence of inorganic surfaces, 40 kerogen fragments were dissolved initially in excess of CO_2 or CH_4 molecules and simulated under NVT ensemble for 40 ns **(see Figure S6)**. In the presence of solid surface, an inorganic surface and 40 kerogen fragments are places at the ends of the simulation box and separated by 10 nm mesopores filled with CO_2 or CH_4 to match the approach applied for the original simulations **(Figure 1).** The governed data from these simulations are represented in **Figure 9**. The main kerogen-kerogen orientation is the π-π stacking with a few T-shape stacking forms **(see Figure S7)**.

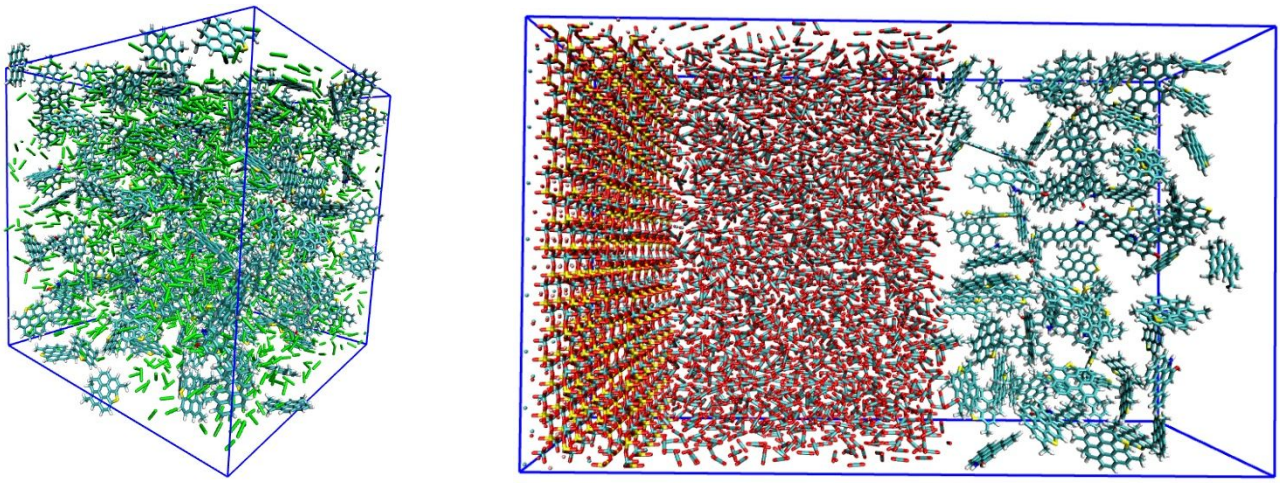

Figure S6. The simulation setup of the kerogen self-assembly in the absence of inorganic surface (left) and in the presence of solid surface (right).

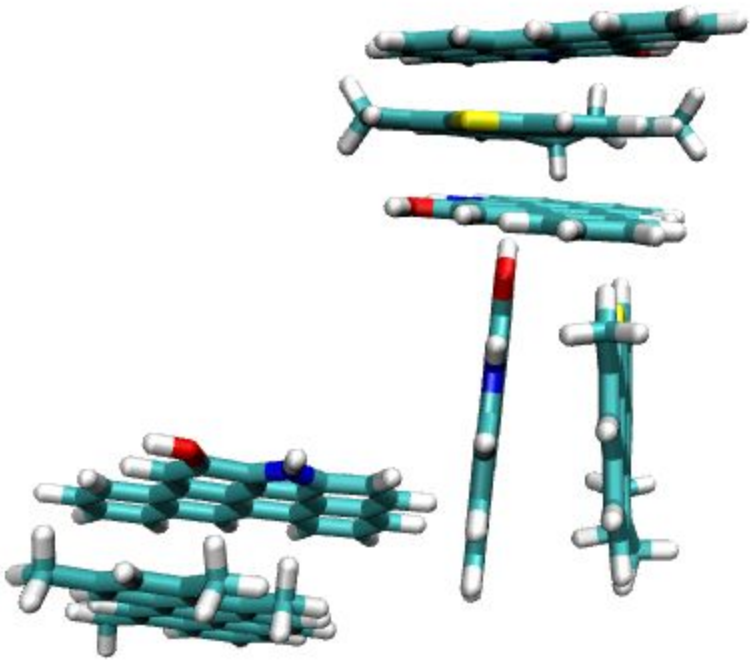

Figure S7. A snapshot of self-assembled kerogen fragments contains $\pi - \pi$ and T-shape stacking.

S5. The diffusion coefficient of CO_2 and CH_4

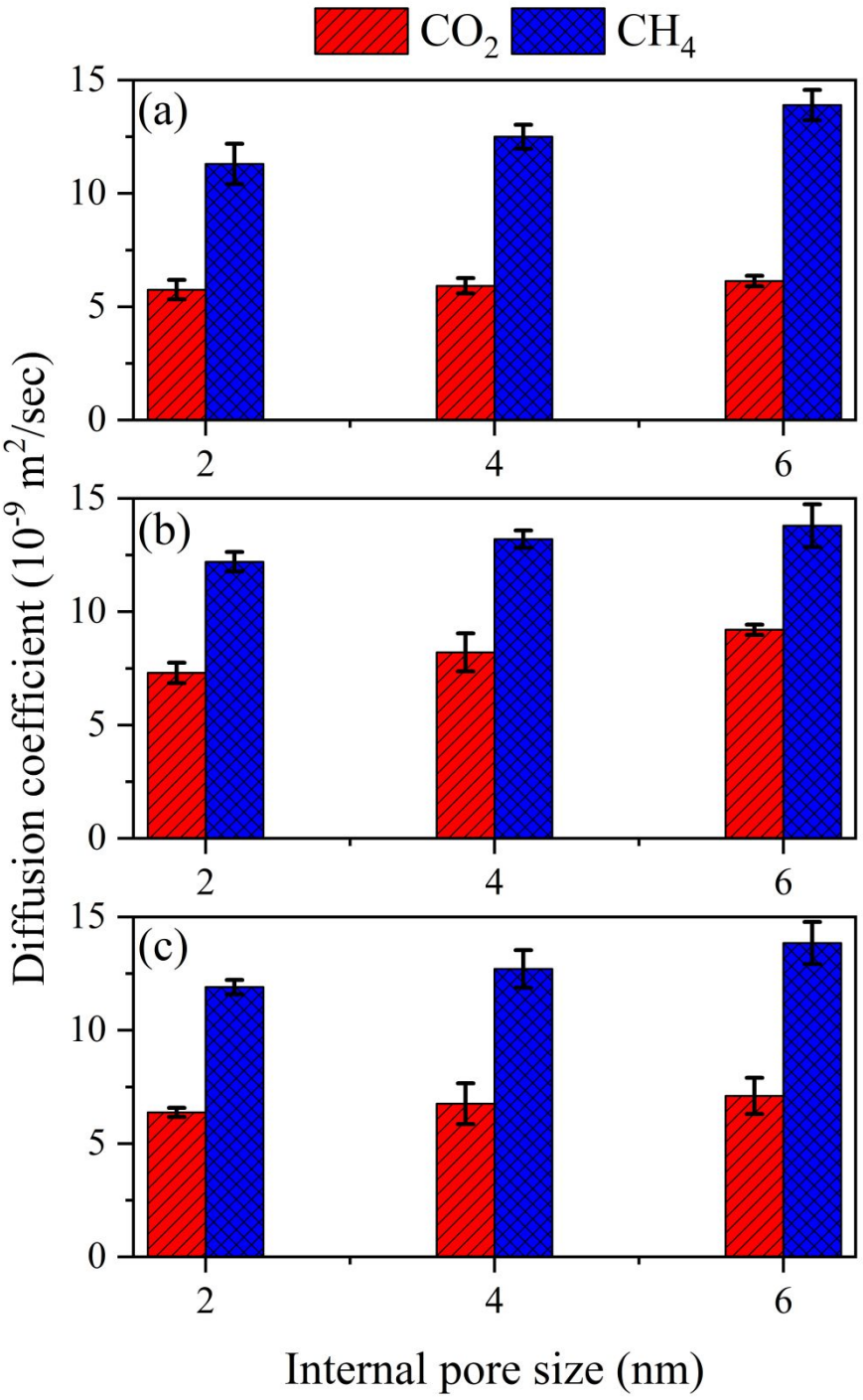

Figure S8. The diffusion coefficient for CO_2 and CH_4 as a function of the nanopore size in the systems composed of (a) calcite/kerogen, (b) silica/kerogen and (c) illite/kerogen. The self-diffusion coefficients were calculated three times during the last 10 ns of the simulation time and the error bars represent the deviation from the average value.

Table S1. The effective surface area and volume of the simulated surfaces as a function of the internal pore diameter.

Surface	Pore size (nm)	Surface area (nm^2)	Volume (nm^3)
Silica	2	172.43 ± 1.4	108.81 ± 1.2
	4	172.43 ± 1.4	217.62 ± 1.4
	6	172.43 ± 1.4	326.43 ± 1.5
Illite	2	325.42 ± 1.8	222.88 ± 2.1
	4	325.42 ± 1.8	445.76 ± 1.8
	6	325.42 ± 1.8	668.64 ± 2.0
Calcite	2	176.62 ± 1.3	112.34 ± 1.1
	4	176.62 ± 1.3	224.56 ± 1.4
	6	176.62 ± 1.3	336.86 ± 0.9
Kerogen	2	534.52 ± 2.7	325.43 ± 2.8
	4	534.52 ± 2.7	650.86 ± 2.3
	6	534.52 ± 2.7	976.29 ± 3.1

References

1. Hao, Y.; Yuan, L.; Li, P.; Zhao, W.; Li, D.; Lu, D. Molecular simulations of methane adsorption behavior in illite nanopores considering basal and edge surfaces. *Energy Fuels* **2018,** *32* (4), 4783-4796.

2. Caineng, Z.; Zhi, Y.; Jingwei, C.; Rukai, Z.; Lianhua, H.; Shizhen, T.; Xuanjun, Y.; Songtao, W.; Senhu, L.; Lan, W.; Bin, B. Formation mechanism, geological characteristics and development strategy of nonmarine shale oil in China. *Petrol. Explor. Dev.* **2013,** *40* (1), 15-27.

3. Sun, H.; Zhao, H.; Qi, N.; Li, Y. Molecular Insights into the Enhanced Shale Gas Recovery by Carbon Dioxide in Kerogen Slit Nanopores. *J. Phys. Chem. C* **2017,** *121* (18), 10233-10241.